Mapping isoprene emissions over North America using formaldehyde column observations from space

Paul I. Palmer, Daniel J. Jacob, Arlene M. Fiore, and Randall V. Martin
Division of Engineering and Applied Sciences, Harvard University, Cambridge, Massachusetts, USA

Kelly Chance and Thomas P. Kurosu
Atomic and Molecular Physics Divisions, Harvard-Smithsonian Center for Astrophysics, Cambridge, Massachusetts, USA

Received 30 January 2002; revised 24 May 2002; accepted 24 July 2002; published 20 March 2003.

[1] We present a methodology for deriving emissions of volatile organic compounds (VOC) using space-based column observations of formaldehyde (HCHO) and apply it to data from the Global Ozone Monitoring Experiment (GOME) satellite instrument over North America during July 1996. The HCHO column is related to local VOC emissions, with a spatial smearing that increases with the VOC lifetime. Isoprene is the dominant HCHO precursor over North America in summer, and its lifetime ($\simeq$1 hour) is sufficiently short that the smearing can be neglected. We use the Goddard Earth Observing System global 3-D model of tropospheric chemistry (GEOS-CHEM) to derive the relationship between isoprene emissions and HCHO columns over North America and use these relationships to convert the GOME HCHO columns to isoprene emissions. We also use the GEOS-CHEM model as an intermediary to validate the GOME HCHO column measurements by comparison with in situ observations. The GEOS-CHEM model including the Global Emissions Inventory Activity (GEIA) isoprene emission inventory provides a good simulation of both the GOME data ($r^2 = 0.69$, $n = 756$, bias = +11%) and the in situ summertime HCHO measurements over North America ($r^2 = 0.47$, $n = 10$, bias = -3%). The GOME observations show high values over regions of known high isoprene emissions and a day-to-day variability that is consistent with the temperature dependence of isoprene emission. Isoprene emissions inferred from the GOME data are 20% less than GEIA on average over North America and twice those from the U.S. EPA Biogenic Emissions Inventory System (BEIS2) inventory. The GOME isoprene inventory when implemented in the GEOS-CHEM model provides a better simulation of the HCHO in situ measurements than either GEIA or BEIS2 ($r^2 = 0.71$, $n = 10$, bias = -10%). *INDEX TERMS:* 0312 Atmospheric Composition and Structure: Air/sea constituent fluxes (3339, 4504); 0345 Atmospheric Composition and Structure: Pollution—urban and regional (0305); 0365 Atmospheric Composition and Structure: Troposphere—composition and chemistry; 0394 Atmospheric Composition and Structure: Instruments and techniques; 0399 Atmospheric Composition and Structure: General or miscellaneous; *KEYWORDS:* Isoprene, Formaldehyde, GOME, biogenic emissions, satellite instrument, volatile organic compounds

Citation: Palmer, P. I., D. J. Jacob, A. M. Fiore, R. V. Martin, K. Chance, and T. P. Kurosu, Mapping isoprene emissions over North America using formaldehyde column observations from space, *J. Geophys. Res.*, *108*(D6), 4180, doi:10.1029/2002JD002153, 2003.

1. Introduction

[2] Formaldehyde (HCHO) columns measured from space by the Global Ozone Monitoring Experiment (GOME) have been reported by *Chance et al.* [2000] and *Palmer et al.* [2001]. As pointed out by *Palmer et al.* [2001], these observations provide a proxy for mapping emissions of volatile organic compounds (VOCs) which are critical for understanding radical chemistry in the troposphere. For this purpose it is essential to (1) evaluate the accuracy of the GOME observations of HCHO columns by comparison with in situ observations and (2) derive the relationship between HCHO columns and VOC emissions. We address here these issues and go on to derive an isoprene emission inventory for North America which we compare to previous estimates from the Global Emissions Inventory Activity (GEIA) [*Guenther et al.*, 1995] and from the second version of the Biogenic Emissions Inventory System (BEIS2) [*Pierce et al.*, 1998].

[3] HCHO is produced in the atmosphere by VOC oxidation. Oxidation of methane (CH_4) provides a global background. In continental boundary layers, oxidation of short-lived VOCs dominates over the source from CH_4 and results in a major enhancement of the total HCHO column. Anthropogenic sources of VOCs are important in urban environments but biogenic sources usually dominate elsewhere, at least during the growing season. The most

0148-0227/03/2002JD002153$09.00

Table 1. In Situ HCHO Measurements Between June and September Over North America[a]

Site	Location [°]	Month Year	Concentration [ppbv]	Statistic	Reference
Surface					
A: Scotia, PA	41°N, 78°W	July and August 1988	4.3 ± 2.0	10–12 LT mean and SD	*Martin et al.* [1991]
B: Egbert, Ontario	44°N, 80°W	July and August 1988	2.1	10–12 LT mean	*Shepson et al.* [1991]
C: Dorset, Ontario	45°N, 79°W	July and August 1988	2.5	10–12 LT mean	*Shepson et al.* [1991]
D: Sarnia, Ontario	42°N, 82°W	June and July 1984	2.5	10–12 LT mean	*Harris et al.* [1989]
E: Cold Creek, Ontario	42°N, 79°W	July 1985	1.2–3.0	range	*Harris et al.* [1989]
F: Research Triangle Park, NC	36°N, 80°W	24–26 June 1986	1.0–9.0	range	*Kleindienst et al.* [1988]
G: Fritz Peak, CO (altitude: 2676 m)	40°N, 105°W	August and September 1993	1.3 ± 0.3	10–14 LT mean and SD	*Fried et al.* [1997]
H: Metter, GA	32°N, 82°W	July and August 1991	3.6	14–16 LT median	*Lee et al.* [1995]
I: Metter, GA		June 1992	3.1	14–16 LT median	*Lee et al.* [1995]
J: Nashville, TN	36°N, 86°W	June and July 1995	11.7	10–20 LT mean	*Riemer et al.* [1998]
K: Fort Leonard Wood, MO	38°N, 92°W	July 1998	7–15	range 9–19 LT	OZIE Campaign (A. Guenther, NCAR, personal communication, 2001)
Aircraft					
L: Nashville, TN	36°–38°N, 85°–89°W	June and July 1995	4.0	median (<2000 m)	*Lee et al.* [1998]

[a]LT denotes local time at the measurement site.

important biogenic VOC is isoprene (CH_2=CH-C(CH_3)=CH_2), which has a lifetime of less than an hour against atmospheric oxidation and produces HCHO with a high yield [*Sprengnether et al.*, 2002].

[4] The atmospheric lifetime of HCHO, determined by losses from photolysis and reaction with the hydroxyl radical (OH), is of the order of a few hours. Correlation of the HCHO column distribution measured by GOME with the emission field of the parent VOCs thus depends on the VOC lifetime, on the HCHO yield from VOC oxidation, and on the HCHO lifetime. Non-zero lifetimes for both the parent VOCs and for HCHO result in smearing and displacement of the correlation, as discussed below.

[5] GOME is a nadir-viewing UV/Vis solar backscatter instrument aboard the European Remote-Sensing-2 satellite, launched in 1995 [*Burrows et al.*, 1999]. The satellite is in a Sun-synchronous orbit, crossing the equator at about 10:30 local solar time (LT) in the descending node. Spectra are collected for three forward scans of the Earth: east, center, and west, each with a pixel size (''footprint'') of 40 × 320 km^2. Full mapping of the globe is achieved in 3 days. The backscattered spectra include a major HCHO absorption region (337–356 nm), whose features have been fitted to reference spectra to retrieve slant columns [*Chance et al.*, 2000]. The slant columns have been converted to vertical columns with an air mass factor (AMF) formulation, constrained for the Rayleigh scattering atmosphere with information on the local shape of the HCHO vertical profile from the Goddard Earth Observing System global 3-D model of tropospheric chemistry (GEOS-CHEM) driven by assimilated meteorological observations [*Palmer et al.*, 2001]. In continental atmospheres most of the HCHO column is in the boundary layer [*Palmer et al.*, 2001].

[6] The GOME HCHO columns over North America in summer show a regional maximum over the southeastern United States, consistent with a major source from oxidation of isoprene [*Lee et al.*, 1995]. Comparison of the GOME and GEOS-CHEM HCHO columns shows a high degree of correlation ($r = 0.77$) with a small positive bias in the model ($\simeq$10%).

[7] An important component of this paper is to assess the accuracy of the GOME HCHO column data. No specific validation experiments have been conducted for that purpose. In situ HCHO measurements from the ground, and, to a lesser extent, from aircraft are available but not coincident with GOME overpasses. We will use here the GEOS-CHEM model as an intermediary for testing the consistency between the in situ and satellite observations over North America in summer, where a large database of in situ measurements is available (Table 1).

[8] Section 2 of this paper describes the theoretical basis for relating HCHO columns to VOC emissions and presents the transfer functions between the two from the GEOS-CHEM model. Section 3 assesses the validity of the GOME data by comparison with in situ observations, and section 4 derives the isoprene emission inventory constructed from the GOME data. Conclusions are in section 5.

2. Deriving VOC Emissions From HCHO Column Measurements

2.1. Production of HCHO From Atmospheric Oxidation of VOCs

[9] VOCs emitted to the atmosphere are oxidized photochemically by a succession of steps leading eventually to CO_2 and H_2O. HCHO is a high-yield intermediate of this oxidation chain. Laboratory chamber data are available for the HCHO yield from oxidation of many VOCs in atmospheres with high concentrations of nitrogen oxides (NO_x = NO + NO_2). In the general case of the oxidation of a hydrocarbon (RH) by OH, the organic peroxy radical (RO_2) produced in the first stage of oxidation reacts with NO, producing HCHO or higher carbonyls that subsequently react to eventually yield HCHO [*Atkinson*, 1994]. In this manner one obtains ultimate HCHO yields per unit carbon of 1 for CH_4 and typically 0.3–1 for C_2–C_6 VOCs

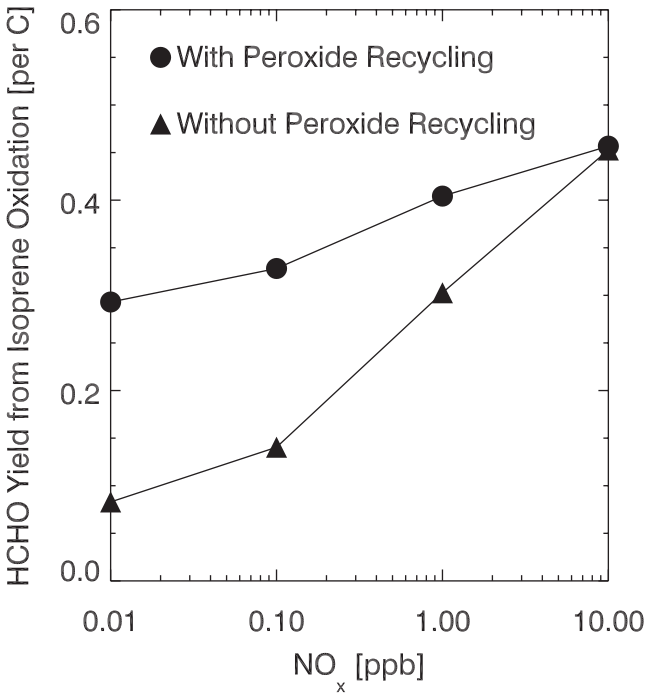

Figure 1. Ultimate HCHO yield per unit carbon from isoprene oxidation as a function of NO_x concentration, as computed in a box model using the isoprene oxidation mechanism from the GEOS-CHEM model (see the study of *Horowitz et al.* [1998], with minor modifications) and assuming chemical steady state for isoprene oxidation intermediates. The calculation is for midday, midlatitude summertime conditions, with 1 ppb isoprene as the only hydrocarbon, 40 ppb O_3, and 100 ppb CO. Results are shown for the mechanism including or excluding chemical recycling of the organic peroxides produced from isoprene oxidation (see text). Excluding chemical recycling effectively assumes that the peroxides are scavenged.

[*Altshuller*, 1991]. Yields less than unity reflect mainly the formation of peroxyacyl radicals RC(O)OO for which further reaction with NO, followed by cleavage, converts the α carbon to CO_2. The HCHO yield per unit carbon from the first stage of isoprene oxidation has been measured in several laboratory studies and found to be in the range 0.11–0.13 [*Sprengnether et al.*, 2002]. Subsequent oxidation of short-lived isoprene oxidation intermediates results in an ultimate yield of about 0.4 per unit carbon from isoprene oxidation (Figure 1). For larger VOCs, including in particular terpenes, HCHO yields are expected to be lower due to formation of organic aerosols from low-volatility oxidation intermediates [*Kamens et al.*, 1982; *Hatakeyama et al.*, 1991; *Orlando et al.*, 2000].

[10] Table 2 lists summertime emission estimates *E* and HCHO oxidation yields *Y* for oxidation by OH under high NO_x conditions of major VOCs emitted in North America. High NO_x conditions, defined here by dominance of reaction with NO as a sink for RO_2 radicals, typically require NO_x concentrations in excess of a few hundred pptv; such conditions are typical of much of the United States but the complications associated with low NO_x conditions will be discussed below. Unless otherwise indicated, the emissions are from the GEOS-CHEM model (Appendix A) and the yields are from the GEOS-CHEM chemical mechanism [*Horowitz et al.*, 1998]. The yields are, in general, close or identical to the values given by *Altshuller* [1991]. The HCHO yield from oxidation of isoprene in the GEOS-CHEM mechanism is based largely on the study of *Paulson and Seinfeld* [1992]. The calculation of HCHO yields in Table 2 sums the contributions from successive stages of VOC oxidation until intermediates with lifetimes in excess of a few days are produced, because further HCHO production is not collocated with the loss of the parent VOC and therefore cannot be readily related to VOC emissions. This explains the low HCHO yield in Table 2 from oxidation of propane and methylbutenol (MBO), for which acetone (lifetime of weeks) represents the dominant first-stage oxidation product. Note also in Table 2 the low HCHO yields from pinenes due to formation of organic aerosol products [*Griffin et al.*, 1999]. Although these compounds make an important contribution to biogenic VOC emissions, they make little contribution to HCHO columns.

[11] The product *YE* measures the column production of HCHO from a given VOC. From Table 2, we see that this production from North America emissions in summer is largely dominated by isoprene, methane, and methanol. Methane is well mixed in the atmosphere because of its long lifetime and defines the HCHO background. Methanol has a lifetime of several days so that the resulting HCHO production is highly dispersed. Isoprene has a lifetime of the order of an hour and a large regional variability in emission [*Guenther et al.*, 1995], so that we expect the variability of HCHO columns over North America in summer to reflect that of isoprene emissions. We elaborate on this point in section 2.2.

[12] One complication in quantifying the yield of HCHO from VOC oxidation is the fate of the RO_2 radicals under low NO_x conditions. Reaction of RO_2 with HO_2 can then compete with reaction of RO_2 with NO and form organic hydroperoxides (ROOH). The main sinks for the simple alkylhydroperoxides are photolysis and reaction with OH on a timescale of hours to days, leading to carbonyl generation with no loss of carbon and not affecting the ultimate HCHO yield [*Lurmann et al.*, 1986]. However, peroxides produced from the oxidation of isoprene by OH have a β-hydroxy group that may increase their solubility in water by several orders of magnitude [*Betterton*, 1992]. Scavenging of these peroxides from the atmosphere would greatly reduce the ultimate HCHO yield from isoprene oxidation under low NO_x conditions (Figure 1) and also represent a major sink for HO_x radicals [*Horowitz et al.*, 1998]. A recent analysis of the HO_x radical budget at an eastern U.S. site in summer indicates that the organic peroxides produced from isoprene oxidation do not represent major sinks of HO_x [*Thornton et al.*, 2002]. We therefore assume (following the study of *Lurmann et al.* [1986]) that these peroxides photolyze and react with OH on a timescale similar to the alkylhydroperoxides, recycling the carbon. In that case, the HCHO yield from isoprene oxidation does not vary much with the NO_x concentration or other variables (Figure 1).

[13] As shown in Figure 1, the ultimate HCHO yield per unit carbon from isoprene oxidation, determined in a photochemical steady-state calculation with the GEOS-CHEM

Table 2. Emission of VOCs and Production of HCHO Over North America in Summer

Species	Emission[a] E (Tg C month^{-1})	Lifetime[b]	HCHO Yield[c] Y (per C reacted)	Potential HCHO Production[d] [%]
Methane	2.6[e]	1 year	1.0	28.5
Ethane	0.15	10 days	0.54	0.9
Propane	0.15	2 days	0.2	0.3
$\geq C_4$ alkanes	0.75	1 day[f]	0.5[f]	4.1
Ethene	0.38	6 hours	0.89	3.7
Propene	0.33	1.5 hours	0.65	2.4
Isoprene	7.3[g]	35 min	0.45	32
α-Pinene	1.1[g]	1 hour	0.019	0.2
β-Pinene	0.8[g]	40 min	0.045	0.4
Methylbutenol	0.8[g]	1 hour[h]	0.13[i]	0.5
HCHO	0.15[g]	2 hours	1.0	1.6
Acetone	0.33	10 days	0.67	2.4
Methanol	2.17[g]	2 days	1.0	23

[a]Emissions are for the North American domain (10°–70°N, 60°–130°W). Values are from the GEOS-CHEM model for July 1996, unless otherwise stated.

[b]VOC lifetimes against oxidation under midmorning summer conditions, assuming [OH] = 5×10^6 mol cm^{-3}, [O_3] = 40 ppb, and a temperature of 298 K. Oxidation by O_3 contributes 25% of the total sink for α-pinene, 8% for propene, and less than 5% for the other VOCs in the table.

[c]Yield from oxidation of VOC by OH under high NO_x conditions (see text), calculated from the GEOS-CHEM chemical mechanism [*Horowitz et al.*, 1998], unless otherwise stated. Ozonolysis represents a minor sink for the pinenes during the daytime [*Atkinson*, 1994] and the associated HCHO yield is expected to be very low [*Orlando et al.*, 2000].

[d]Relative contribution from the VOC to the total HCHO production from North American emissions as determined by $Y_iE_i/\Sigma_jY_jE_j$ where the sum is over all emitted VOCs.

[e]Estimate from the *U.S. Department of Energy* [1997].

[f]For *n*-butane.

[g]Estimates based on annual biogenic emissions from the study of *Guenther et al.* [2000], assuming that July accounts for 25% of total annual emissions (GEOS-CHEM model result for isoprene).

[h]Calculated value assumes a reaction rate of 64×10^{-12} cm^3 molecules^{-1} s^{-1} [*Alvarado et al.*, 1999] based on measured values from the study of *Rudich et al.* [1995]. MBO also reacts with O_3 but this represents a minor sink during the daytime [*Atkinson and Arey*, 1998].

[i]*Alvarado et al.* [1999] report molar yields of 0.29 HCHO, 0.19 $(CH_3)C(OH)CHO$, 0.61 $CH_2(OH)CHO$, 0.58 acetone, and 0.05 organic nitrate in the first stage of methylbutenol oxidation by OH under high NO_x conditions. Subsequent photolysis and oxidation of $(CH_3)C(OH)CHO$ and $CH_2(OH)CHO$ in our mechanism under high NO_x conditions produce HCHO with molar yields of 0.25 and 0.50, respectively, resulting in an overall HCHO yield of 0.13 per atom C from the oxidation of MBO.

model mechanism, is 0.3–0.45. Results from a time-dependent calculation with the same mechanism (Figure 2) provide insight into how the HCHO yield from isoprene oxidation increases with time. At high NO_x concentrations (1 ppb), 90% of the ultimate HCHO yield (0.43 per C) is reached within the first 2 hours. At the low NO_x concentrations (0.1 ppb) only 55% of the ultimate HCHO yield (0.29 per C) is reached in the same time period because of the formation of the peroxide reservoir; 2 days are required to reach 90% of the ultimate HCHO yield. Thus, we may expect a better correlation of HCHO columns with isoprene emissions in the high-NO_x than in the low-NO_x regime. This is further discussed in section 2.3 in the context of GEOS-CHEM model results.

2.2. Relating HCHO Columns to VOC Emissions

[14] Consider an atmospheric HCHO column Ω (molecules cm^{-2}) produced from the oxidation of an ensemble of VOCs (VOC$_i$, $i = 1, \ldots, n$) with emission fluxes E_i (atoms C cm^{-2} s^{-1}) and HCHO yields Y_i per C atom. Let k_{HCHO} (s^{-1}) represent the loss rate constant for HCHO in the column from oxidation and photolysis. In the absence of horizontal transport, Ω at steady state would be given by

$$\Omega = \frac{1}{k_{\mathrm{HCHO}}} \sum_i Y_i E_i, \tag{1}$$

so that measurement of Ω would provide a proxy for the sum of local VOC emissions weighted by the HCHO yield. Horizontal transport displaces and smears this signal. Consider an air column (for all practical purposes the boundary layer) with mean column wind speed U in which a puff of VOC$_i$ with loss rate constant k_i is injected at a certain location. Let us assume that HCHO is produced in the first stage of oxidation or quickly thereafter (i.e., from short-lived intermediates) so that we can write

$$\mathrm{VOC}_i \xrightarrow{k_i} Y_i \mathrm{HCHO} \tag{2}$$

[15] By solving the mass balance equations for VOC$_i$ and HCHO in the air column one finds that the maximum in the HCHO column produced from the VOC$_i$ emission puff is located downwind from the point of emission at a displacement length scale $L_{d,i}$ given by

$$L_{d,i} = \frac{U}{k_i - k_{\mathrm{HCHO}}} \ln\left(\frac{k_i}{k_{\mathrm{HCHO}}}\right). \tag{3}$$

[16] One can further define a smearing length scale $L_{s,i}$ as the distance where the integral of Ω downwind of the point of emission, $\int_0^{L_{s,i}} \Omega dx$, reaches a fraction $(1 - 1/e)$ of its asymptotic value $\int_0^{\infty} \Omega dx = [\mathrm{VOC}]_0/k_{\mathrm{HCHO}}$, where

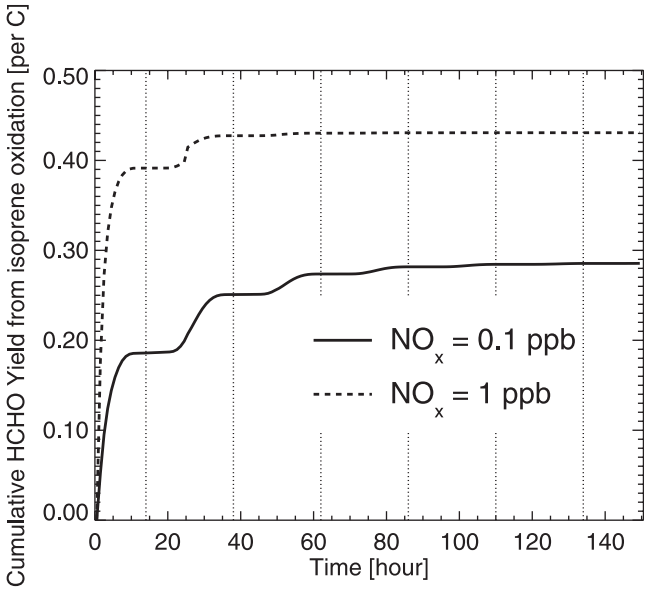

Figure 2. Cumulative HCHO yield per unit carbon from isoprene oxidation as a function of time, computed in a photochemical box model using the isoprene oxidation mechanism from the GEOS-CHEM model with peroxide recycling. The calculation is initialized at 9 LT for midlatitude summertime conditions, with 1 ppb isoprene as the only hydrocarbon, 40 ppb O_3, 100 ppb CO, and either 0.1 or 1.0 ppb of NO_x. Isoprene is allowed to decay while O_3, CO and NO_x are held are their initial values. Vertical lines denote midnight of each day.

$[VOC]_0$ is the initial VOC column concentration at the point of emission. From solution to the mass balance equations one finds that $L_{s,i}$ is the solution of the transcendental equation

$$\frac{1}{k_{\mathrm{HCHO}} - k_i}\left(k_{\mathrm{HCHO}} \exp\left[\frac{-k_i L_{s,i}}{U}\right] - k_i \exp\left[\frac{-k_{\mathrm{HCHO}} L_{s,i}}{U}\right]\right) - \frac{1}{e} = 0, \tag{4}$$

with limiting values $L_{s,i} \rightarrow U/k_i$ when $k_i \ll k_{\mathrm{HCHO}}$, and $L_{s,i} \rightarrow U/k_{\mathrm{HCHO}}$ when $k_{\mathrm{HCHO}} \ll k_i$.

[17] For isoprene, a typical lifetime against oxidation by OH in late morning is 0.5 hour, i.e., $k_i = 2\ \mathrm{h}^{-1}$. Further assuming typical values $k_{\mathrm{HCHO}} = 0.5\ \mathrm{h}^{-1}$ and $U = 20$ km h^{-1} we obtain $L_{d,i} = 20$ km and $L_{s,i} = 50$ km. For methane (lifetime of several years) and methanol (lifetime of several days), $L_{s,i}$ values are sufficiently large that there is no spatial resolution to the HCHO signal. We conclude that the HCHO column seen by GOME over North America in summer should map isoprene emissions with a spatial resolution of the order of 10–100 km. This resolution is comparable to the size of the GOME pixel (320×40 km^2) so that for practical purposes we can view variability in the HCHO columns observed by GOME as reflecting local isoprene emission. In an alternate situation where VOCs with lifetimes of days made a major contribution to HCHO columns, as would be expected for example in winter, then the smearing length scale would be of the order of 1000 km. Relating the observed HCHO columns to VOC emissions would then require a complicated inversion.

2.3. 3-D Model Analysis

[18] The above ideas, including in particular the relationship between measured HCHO column and local isoprene emission, can be tested using the GEOS-CHEM global 3-D model of tropospheric chemistry (Appendix A). A general description of the model is given by *Bey et al.* [2001], and specific applications to O_3–NO_x–VOC chemistry over North America in summertime are given by *Palmer et al.* [2001], *Fiore et al.* [2002], and *Li et al.* [2002]. This model includes emissions from anthropogenic alkanes, anthropogenic and biogenic alkenes, acetone, and isoprene (Table 2). Isoprene emission in our standard simulation is from the GEIA inventory [*Guenther et al.*, 1995] but we will also show results from a sensitivity simulation using the BEIS2 inventory [*Pierce et al.*, 1998]. The horizontal resolution is $2^\circ \times 2.5^\circ$ ($\simeq$200 km), so that mesoscale displacement and smearing of the HCHO column resulting from isoprene emission are not resolved, as is the case also for GOME.

[19] We plot in Figure 3 the GEOS-CHEM relationship between HCHO columns and local isoprene emission in late morning (10–12 LT) for grid squares sampled along the GOME orbit tracks over the United States during July 1996.

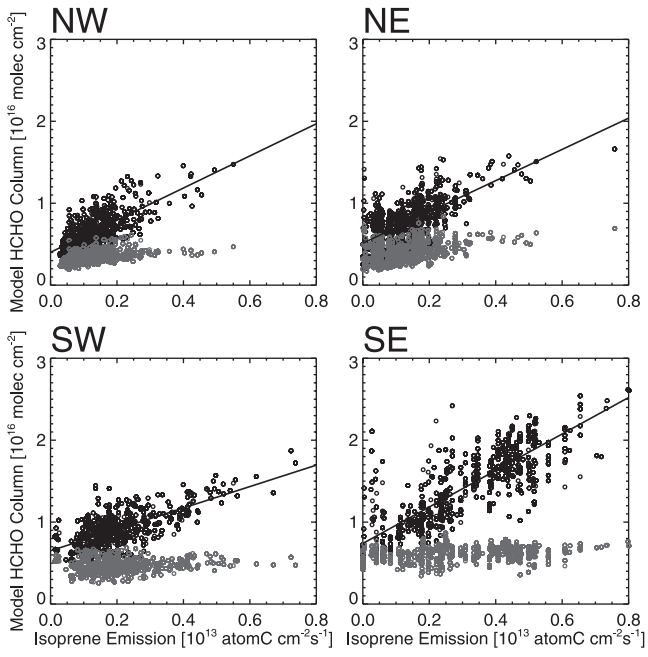

Figure 3. Relationship between isoprene emissions and HCHO columns in the GEOS-CHEM model for July 1996 over North America (25°–50°N, 65°–130°W) at 10–12 LT, partitioned by quadrants with longitudinal and latitudinal divides at 100°W and 40°N. Model values are sampled along the ensemble of GOME orbit tracks during July 1996. Cloud fraction data from GOME [*Kurosu et al.*, 1999] have been used to filter out scenes with >40% cloud cover. The linear least-squares fit lines are shown and the corresponding statistical data are given in Table 3. The red data points represent HCHO columns from sources other than isoprene, as determined from a sensitivity simulation without isoprene emissions. See color version of this figure at back of this issue.

Table 3. HCHO Lifetimes and Yields From Isoprene Oxidation Over North America During Summer as Calculated From the Data Shown in Figure 3

Quadrant[a]	Number of Points	Slope S[b] [10^3 s]	Intercept[c] [10^{15} molecules cm^{-2}]	r^2	Mean HCHO Column Lifetime [hours]	HCHO Yield[c] From Isoprene [per C]
NW	1810	2.04	4.01	0.51	1.67	0.34
NE	2193	1.90	5.35	0.43	1.76	0.30
SE	1913	2.09	7.82	0.65	1.48	0.39
SW	1750	1.27	6.64	0.49	1.48	0.24

[a]Values are GEOS-CHEM model results sampled along GOME orbit tracks for North America (25°–60°N, 65°–130°W) at 10–12 LT in July 1996, partitioned by quadrants with latitudinal and longitudinal divides at 40°N and 100°W.
[b]Slope, intercept, and coefficient of correlation r^2 of the linear regression for the HCHO column versus isoprene emission relationships in Figure 3.
[c]Apparent HCHO yield Y from isoprene oxidation in the model as determined from $Y = Sk_{HCHO}$, where S is the slope of the HCHO column versus isoprene emission relationship and k_{HCHO} is the inverse of the mean HCHO column lifetime.

A strong linear relationship is found in the ensemble of data, confirming the dominance of isoprene over other model VOCs as source of HCHO and also confirming that $L_{d,i}$ and $L_{s,i}$ for isoprene are indeed small relative to the 2° × 2.5° resolution of the model. Also shown in Figure 3 are the contributions to the HCHO columns from sources other than isoprene, as determined from a simulation without isoprene emissions. We see that other VOCs make little contribution to HCHO enhancements over North America in the model and do not alias significantly the correlation of HCHO columns with isoprene emissions.

[20] It follows from the above arguments that the slope of the linear relationship between HCHO column and isoprene emission in Figure 3 should roughly equal Y/k_{HCHO} (from (1)), where Y is the HCHO yield from isoprene oxidation. Mean values of the mean HCHO column lifetime ($1/k_{HCHO}$) for each North American quadrant at 10–12 LT, as calculated in GEOS-CHEM, are given in Table 3. The values for the slopes imply HCHO yields in the range 0.24–0.39 (Table 3) from the oxidation of isoprene in the model, consistent with the values derived from the chemical mechanism (Table 2 and Figure 1), and confirming the robustness of the overall approach. The apparent low yield computed for the SW is due to the effect of smearing in a highly heterogeneous isoprene emission field. The definition of SW and SE quadrants dissects a region of relatively low isoprene emission (SW) and an extremely active isoprene emitting region (SE) (see Figure 4). The related manifestation of this smearing is apparent in the SE quadrant, as an occasional enhancement of the HCHO column over areas without isoprene emissions. In section 4, we will use the model slopes of Figure 3 as a transfer function to convert the HCHO columns observed by GOME into isoprene emission fluxes.

3. Consistency Between GOME and In Situ HCHO Observations

3.1. Updated GOME HCHO Column Data

[21] Since the works of *Chance et al.* [2000] and *Palmer et al.* [2001] we have improved several aspects of the retrieval of GOME HCHO vertical columns from the fitted slant columns. In particular, we have included AMF sensitivity to aerosol extinction by using local aerosol optical depths (AOD) from the GEOS-CHEM model [*Fiore et al.*, 2002]. The AODs at 340 nm over the United States are typically in the range 0.1–1, and are assumed to be

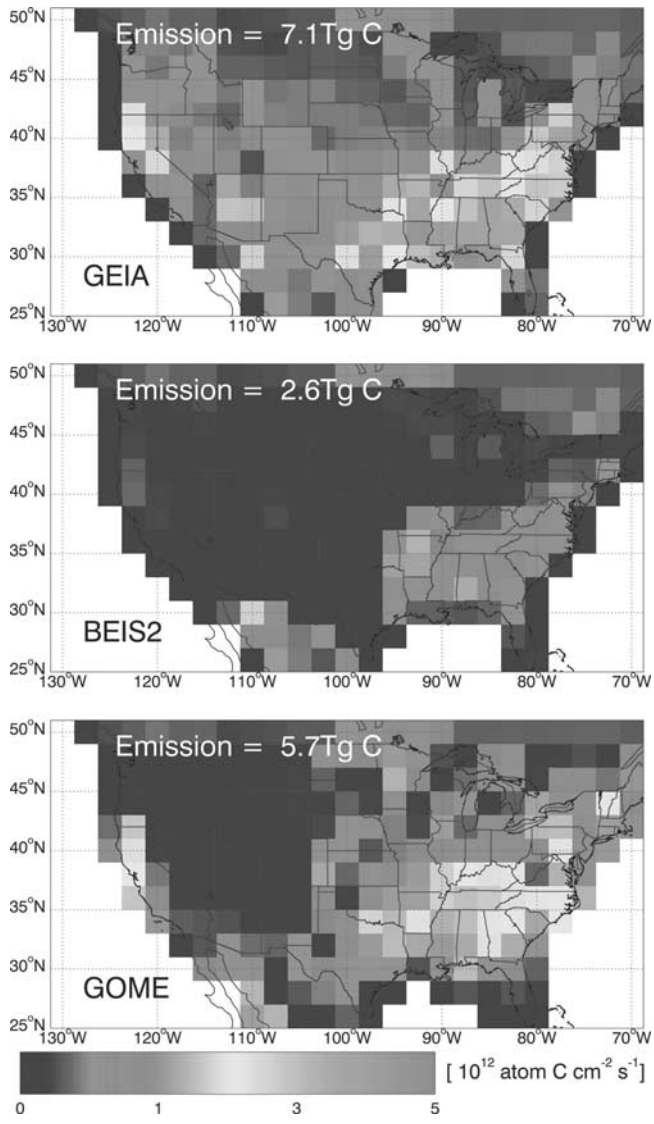

Figure 4. Monthly mean isoprene emission fluxes over North America for July 1996 from the GEIA and BEIS2 inventories and as retrieved from the GOME HCHO column observations. Total isoprene emissions during July over the domain is shown inset. See color version of this figure at back of this issue.

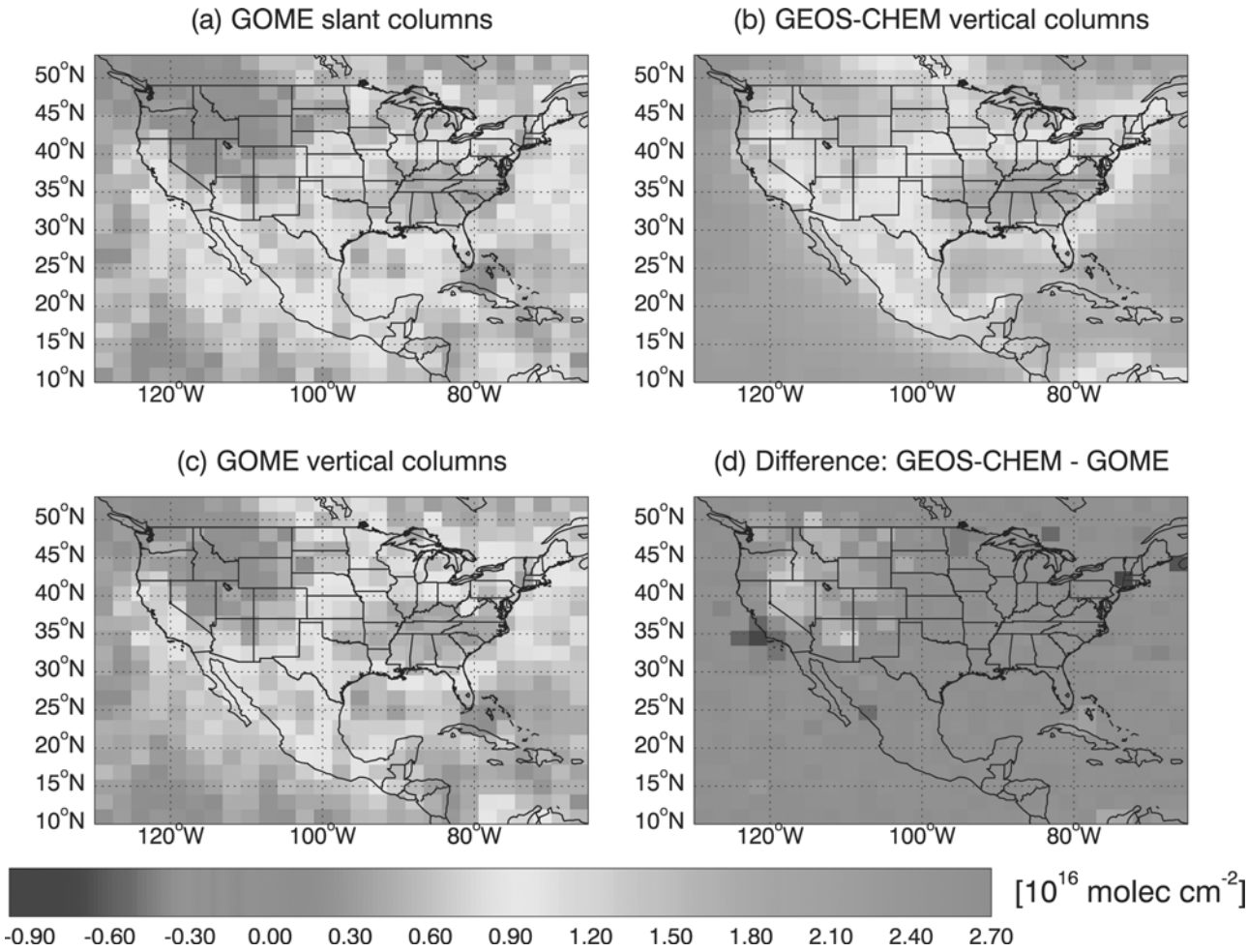

Figure 5. Mean HCHO columns over the United States for July 1996 on a 2° × 2.5° grid. (a) Observed slant columns from GOME [*Chance et al.*, 2000]. (b) Vertical columns from the GEOS-CHEM global 3-D model. (c) Observed vertical columns from GOME after application of the AMF. (d) Differences between modeled and observed vertical columns. Both model and observations are for 10ndash;12 LT and for cloud cover <40% [*Kurosu et al.*, 1999]. See color version of this figure at back of this issue.

uniformly distributed over the depth of the local boundary layer. A single scattering albedo of 0.96 [*Dickerson et al.*, 1997] is assumed. *Palmer et al.* [2001] previously found that increasing the AOD of scattering aerosols from 0.1 to 1.0 (representing a typical AOD range at 340 nm over North America during summertime) increased the GOME sensitivity to the HCHO column by approximately 30% relative to an aerosol-free atmosphere.

[22] Clouds mask boundary layer HCHO from the GOME instrument, introducing a negative bias in the retrieval if not accounted for [*Martin et al.*, 2002]. The GOME footprint (40×320 km^2) is rarely cloud free. *Palmer et al.* [2001] used cloud fraction information for each GOME scene from the Initial Cloud Fitting Algorithm (ICFA) [*Kuze and Chance*, 1994] to exclude data with cloud fraction >40%. This threshold value represents a trade-off between data quality and coverage; using alternative threshold values of 30% or 50% did not alter significantly the results. In this work we use an improved GOME cloud product, the GOME Cloud AlgoriThm (GOMECAT) [*Kurosu et al.*, 1999] to remove scenes with cloud fraction >40%.

[23] Recent work has highlighted an artifact likely introduced by the solar diffuser plate onboard the GOME instrument [*Richter and Wagner*, 2001; *Richter et al.*, 2002; *Martin et al.*, 2002]. The artifact takes the form of a daily varying global bias in the retrieved column. Here we have estimated the effect of the diffuser plate on the HCHO slant column retrieval by first computing 3-day spatial means (GOME provides global coverage every 3 days) during July 1996 over the eastern Pacific (30°–50°N, 140°–180°W) where we would expect HCHO columns to be determined by CH_4 oxidation and relatively constant. We assume the model chemistry to be correct in this remote region and calculate the mean HCHO column in the model for July 1996 to be 3.0×10^{15} molecules cm^{-2}. Subtraction of this model-derived HCHO column from the GOME slant column yields a residual structure, with a mean value of 0.3 $\pm 2 \times 10^{15}$ molecules cm^{-2} during July 1996. This structure is well within the spectral fitting precision of 4×10^{15} molecules cm^{-2} [*Chance et al.*, 2000]. We remove it from the fitted slant columns by assuming that it is globally invariant [*Martin et al.*, 2002].

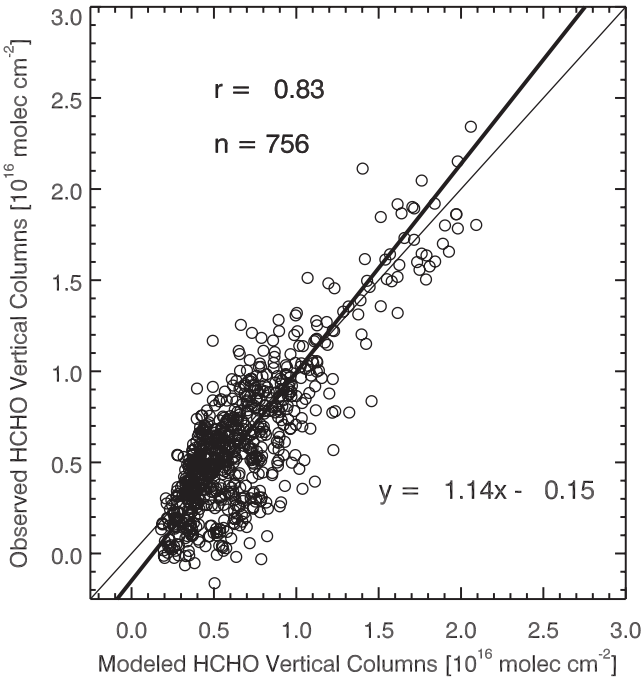

Figure 6. Scatterplot of observed (GOME) and modeled (GEOS-CHEM) monthly mean HCHO vertical columns in July 1996 over the $2^\circ \times 2.5^\circ$ grid shown by Figure 5. The data plotted here are Figure 5c (GOME) and Figure 5b (GEOS-CHEM). The thick and thin solid lines represent the reduced major axis regression line [*Hirsch and Gilroy*, 1984] and the $y = x$ relation, respectively. The Pearson correlation coefficient r and the number of elements n used to compute r are also shown.

[24] Figure 5 shows the monthly mean GOME vertical columns computed with the above updates. As in the study of *Palmer et al.* [2001], the AMF values for converting slant to vertical columns use local HCHO profiles from the GEOS-CHEM model for the position and time of each observation. The GEOS-CHEM model includes a number of minor improvements over the *Palmer et al.* [2001] study, as described in Appendix A. Differences between the results shown here and those presented by *Palmer et al.* [2001] are typically less than 10%. Subtraction of the diffuser plate artifact from the GOME slant columns is the most important effect. Agreement between GOME and GEOS-CHEM monthly mean HCHO columns is slightly improved relative to that shown by *Palmer et al.* [2001]. A scatterplot of the data (Figure 6) shows a Pearson correlation coefficient r of 0.83 (previously 0.77), with a model bias of +11%. We define the percent model bias, following the study of *Balkanski et al.* [1993], as

$$\text{bias} = 100\frac{1}{n}\sum_{i=1}^{n}\frac{\Omega_i^M - \Omega_i^O}{\max(\Omega_i^M, \Omega_i^O)}, \quad (5)$$

where Ω_i^M and Ω_i^O represent the ith model and observed HCHO column, respectively. The variability of HCHO columns in the model is largely driven by emission of isoprene (Figure 3), implying the same for the GOME observations.

3.2. Daily Variability in GOME HCHO Columns

[25] To further diagnose the relationship between GOME columns and isoprene emissions, we examine data from individual GOME orbits. Isoprene emissions from a given location vary from day to day in response to changes in temperature and to a lesser extent solar radiation [*Guenther et al.*, 1995]. The Ozarks Plateau in southeastern Missouri is expected to have unusually high isoprene emissions because of oak forest cover and high temperatures [*Xu et al.*, 1997; A. Guenther, NCAR, personal communication, 2001]. The GOME data show frequent occurrences of very high HCHO columns in that area, with a strong day-to-day variability that is not captured by the model (Figure 7). We examined whether this daily variability observed by GOME over the Ozarks can be interpreted in terms of variability in the meteorological variables determining isoprene emission. Figure 8 shows the daily HCHO slant columns (used instead of vertical columns to avoid any model influence [*Palmer et al.*, 2001]) as a function of surface air temperature. We find that the columns are significantly correlated to surface temperature in a manner that shows some consistency with the exponential temperature dependence of isoprene emission [*Guenther et al.*, 1995]. However, the highest temperatures are not associated with particularly high HCHO columns.

3.3. Consistency With In Situ Observations

[26] Aircraft vertical profiles of HCHO concentrations are available from the Southern Oxidants Study (SOS) over Tennessee in summer 1995 [*Lee et al.*, 1998]. These data were previously compared with simulated GEOS-CHEM profiles by *Palmer et al.* [2001] to evaluate the ability of the model to reproduce the vertical shape factor for the AMF calculation. Here we compare the HCHO columns computed from the aircraft observations to the GOME column observations and to the corresponding GEOS-CHEM model values.

[27] The SOS aircraft data (19 June to 22 July) include 14 vertical profiles in the region 29.3°–40.5°N, 82.4°–105.4°W, extending from 0.1 to 8 km altitude. Model results indicate that HCHO above 8 km contributes less than 5% to the total column, reflecting the absence of short-lived VOCs at these altitudes and the temperature dependence of the oxidation of CH_4. Thus, the aircraft observations (June and July 1995) provide a good approximation to the total HCHO column for comparison with the GOME observations (July 1996) on a statistical basis. The SOS aircraft observations have a mean column value of $2.0 \pm 0.3 \times 10^{16}$ molecules cm^{-2} (14 profiles), while the GEOS-CHEM modeled HCHO columns during July 1995 for the same geographic region have a mean column value of $1.4 \pm 0.2 \times 10^{16}$ molecules cm^{-2}, representing a negative bias of 30%, consistent with previous results [*Palmer et al.*, 2001; *Fiore et al.*, 2002]. The spatial mean of the monthly mean GOME HCHO columns in $2^\circ \times 2.5^\circ$ grid squares over the same geographic region (29.3°–40.5°N, 82.4°–105.4°W) for July 1996 is $1.3 \pm 0.4 \times 10^{16}$ molecules cm^{-2}; whereas the same statistic in the GEOS-CHEM model is $1.4 \pm 0.4 \times 10^{16}$ molecules cm^{-2}. The GOME and GEOS-CHEM HCHO columns are therefore consistent, and 30% lower than the aircraft observations. Most of the discrepancy between the model and the aircraft observations is in the lower free troposphere [*Palmer et al.*,

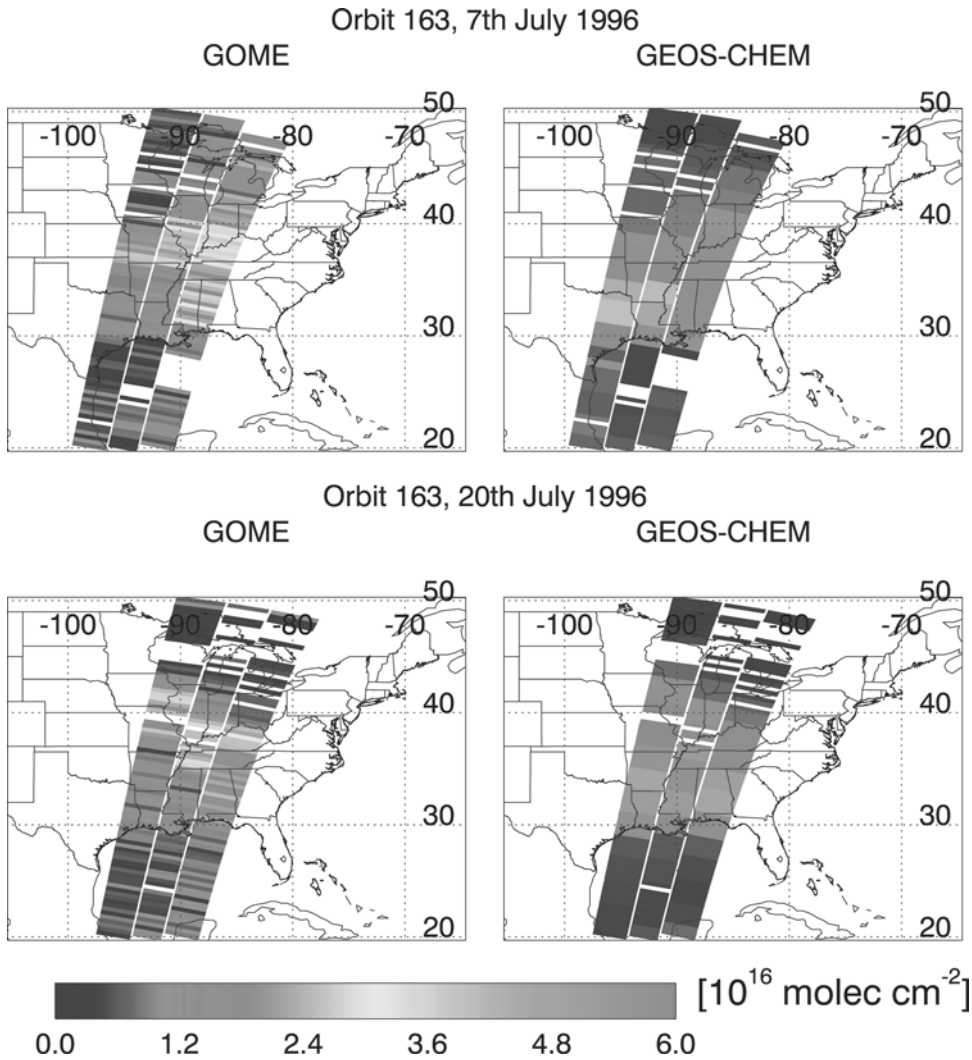

Figure 7. GOME HCHO vertical columns for two sample orbits over North America during July 1996. The left panels are the observed vertical columns and the right panels are the corresponding vertical columns from the GEOS-CHEM model at 10–12 LT. Data with GOMECAT [*Kurosu et al.*, 1999] cloud fraction values >0.4 have been omitted from both modeled and observed scenes. See color version of this figure at back of this issue.

2001] where photochemical models in general tend to yield values lower than observed [*Frost et al.*, 2002].

[28] In situ measurements of HCHO at surface sites in North America (Table 1) bring additional information about the concentration and distribution of HCHO. We cannot compare them directly to the GOME column data, but through comparisons with the GEOS-CHEM model results we can determine whether they are consistent. The measured HCHO concentrations range from 0.1 to 12 ppb, largest in the Southeast United States. We compare in Figure 9 the observed HCHO concentrations from Table 1 with GEOS-CHEM model results using GEIA and BEIS2 inventories for July 1996. Note the large difference between the two inventories (Figure 4), although the spatial correlation between them is significant (r^2 = 0.58). The model is unable to capture the two largest HCHO observations (>6 ppb), corresponding to points J and K. *Riemer et al.* [1998] (point J, see Table 1) report a mean daytime HCHO concentration of 12 ppb in Tennessee during SOS, which they attribute largely to isoprene. Data from the Ozarks site (point K) indicate a range of 7–15 ppb, again reflecting high local isoprene emissions (A. Guenther, NCAR, personal communication, 2001). The Ozarks maximum of isoprene emission is apparent in the BEIS2 inventory [*Pierce et al.*, 1998] but loses definition when averaged over the 2° × 2.5° GEOS-CHEM model grid (Figure 4). Aircraft measurements during the 1999 SOS showed a HCHO increase by more than a factor of 4 when passing over the Ozarks region at an altitude of 500 m (Y.-N. Lee, Brookhaven National Laboratory, personal communication, 2001).

[29] If points J and K are removed from the comparison we find that the model can reproduce most of the variance in the in situ surface air observations (Figure 9). In the standard simulation using the GEIA inventory the reduced major-axis linear regression [*Hirsch and Gilroy*, 1984] approaches the $y = x$ line. When the BEIS2 inventory is used, the model underestimates observations by 30% on average, consistent with the difference in isoprene emis-

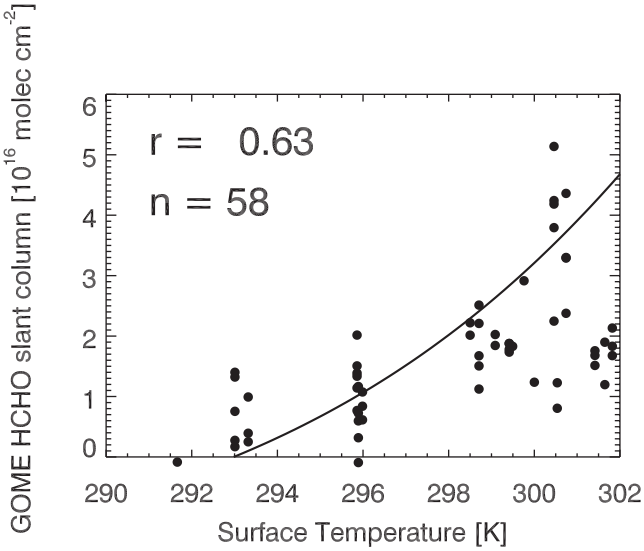

Figure 8. GOME HCHO slant column sensitivity to GEOS surface air temperature over the Ozarks Plateau, Missouri (37°–39°N, 87°–89°). The Pearson correlation coefficient r and the number of elements n used to compute r are also shown. The solid line represents the exponential dependence of isoprene emission on temperature as given by *Guenther et al.* [1995].

sions relative to GEIA. The successful model simulation of both the in situ surface air observations (Figure 9) and the GOME observations (Figure 5) when the GEIA isoprene emissions are used suggests that the GOME data and the in situ observations are consistent.

4. Estimating Isoprene Emissions From GOME HCHO Data

[30] To estimate isoprene emissions from GOME HCHO column data we use the modeled relationships shown in Figure 3, which are discussed in detail in section 2. These linear relationships are transposed to construct a transfer function in which an isoprene emission can be calculated given a HCHO column measurement. The emissions are then regridded on the $2 \times 2.5°$ GEOS-CHEM model grid and local diurnal factors from the GEOS-CHEM simulation are applied to convert the 10–12 LT values to 24-hour averages. Monthly mean emission estimates are then calculated (Figure 4). The spectral fitting uncertainty of 4×10^{15} molecules cm^{-2} on the HCHO columns corresponds to a mean uncertainty for the inferred isoprene emissions to be

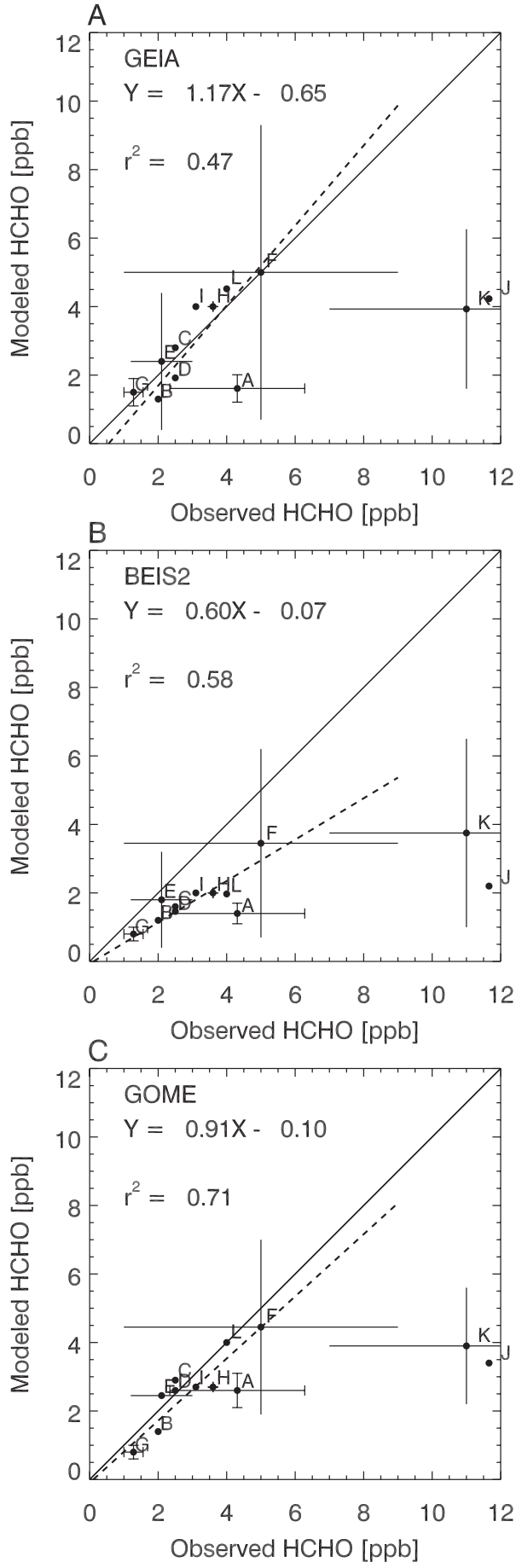

Figure 9. (opposite) Scatterplot of observed and GEOS-CHEM simulated surface HCHO concentrations for the ensemble of sites and statistics compiled in Table 1. Error bars denote either a range of values (open ends) or mean value ± 1σ (closed ends).The three plots correspond to different isoprene emission inventories used in GEOS-CHEM: GEIA, BEIS2, and GOME (see text for details). The solid lines represent the $y = x$ line. The black dashed lines represent the reduced major-axis linear regression lines [*Hirsch and Gilroy*, 1984] fitted to all observations excluding J and K (see text). Pearson correlation coefficients r^2 for fitted observations are inset of each plot.

1.1×10^{12} C cm^{-2} s^{-1}. After monthly averaging we get slight negative isoprene emissions in three $2 \times 2.5°$ grid squares over North America, reflecting HCHO columns well within the HCHO fitting uncertainty. For purposes of applying the GOME isoprene emission inventory to GEOS-CHEM, we set these negative isoprene emissions to zero.

[31] Figure 4 shows that the GOME-derived isoprene emissions over North America in July (5.7 Tg C) are lower than the GEIA emissions (7.1 Tg C), and the spatial distribution shows some differences ($r^2 = 0.41$). In particular, GOME emissions are higher in the midwest and the deep south. The BEIS2 inventory is lower than GOME by a factor of 2 with a spatial r^2 of 0.35. The high GOME values over southern New England could possibly reflect anthropogenic hydrocarbons emitted in the Northeast metropolitan corridor.

[32] Discarding data with >40% cloud cover introduces a bias in the monthly mean isoprene emissions derived from GOME data. We estimated this bias using the model by excluding periods with cloud cover >40% from the monthly mean isoprene emissions computed with the GEIA inventory. The resulting bias range between −20% and −35% over North America during July 1996 and typically smaller than −25%.

[33] To provide closure on the consistency between the GOME HCHO columns and the in situ HCHO data, we conducted a GEOS-CHEM simulation using the GOME-derived isoprene emissions and compared the resulting HCHO concentrations in surface air to the observations in Table 1. Figure 9c shows the results. The GOME emission inventory for isoprene achieves a better simulation of the surface air observations than either GEIA or BEIS2, with less scatter in the comparison. Even with the GOME isoprene emission inventory we are still not able to reproduce the observations at points J and K, which as previously noted could reflect subgrid-scale variability.

5. Summary and Discussion

[34] Accurate VOC emission inventories are essential to understand radical chemistry in the troposphere. Conventional emission inventories for both anthropogenic and biogenic VOCs are highly uncertain. Here we documented a new methodology to obtain VOC emissions from space-based HCHO column observations and applied it to data from the GOME satellite instrument.

[35] HCHO is a high-yield product of VOC oxidation and its lifetime is short enough that a measure of its column abundance should correlate well with the emission field of its parent VOC. In regions with an active biosphere, isoprene is the dominant HCHO precursor. Anthropogenic VOCs could dominate over urban areas but would not be resolved with the GOME footprint (320×40 km^2) Although emissions of terpenes can exceed those of isoprene for some ecosystems, the HCHO yield from terpenes is far less than from isoprene.

[36] We used the GEOS-CHEM global 3-D model of tropospheric chemistry to derive linear relationships between HCHO columns and isoprene emissions over North America in summer for application to GOME. The slope of the relationship in the model implies a HCHO yield of 0.24–0.39 per atom C of isoprene, consistent with a steady state analysis of the model photochemical mechanism, which is, in turn, constrained by laboratory studies of isoprene oxidation products. Smearing and displacement length scales are found to be of little importance when relating HCHO columns to isoprene emissions over the grid resolution of the model ($2 \times 2.5°$).

[37] We presented updated GOME HCHO columns over North America in July 1996 including several minor improvements over the original retrievals of *Chance et al.* [2000] and *Palmer et al.* [2001]. Results were compared to GEOS-CHEM model results with two different isoprene emission inventories, GEIA [*Guenther et al.*, 1995] and BEIS2 [*Pierce et al.*, 1998]. We find that these two inventories, although substantially different (GEIA emissions over North America are almost 3 times higher than BEIS2) both account for about 50% of the spatial variance in the GOME observations. Use of the GEIA isoprene inventory leads to a 3% negative bias in HCHO while the BEIS2 has a 33% negative bias. Summertime statistics of HCHO concentrations measured at surface sites in the United States and Canada are reproduced closely by the GEOS-CHEM model using GEIA emissions, implying consistency between these in situ observations and the GOME columns. Examination of individual GOME orbits reveals occurrences of extremely high HCHO columns over the Ozarks (southeastern Missouri) where isoprene emissions in current inventories are particularly high. The day-to-day variability of GOME HCHO columns over the Ozarks shows some consistency with the temperature dependence of isoprene emission.

[38] The GOME observations were used to construct an isoprene emission inventory for North America which was compared to GEIA and BEIS2 and applied within the GEOS-CHEM model to simulate in situ HCHO observations. This GOME-derived isoprene emission inventory (5.7 Tg C) is comparable to GEIA on the continental scale (7.1 Tg C) but the spatial distribution shows some differences ($r^2 = 0.41$). GOME emission fluxes are higher in the midwest and the deep south. The BEIS2 inventory is lower than GOME by a factor of 2 with a spatial correlation r^2 of 0.35. Applying the GOME-derived isoprene emissions to the GEOS-CHEM model provides a better simulation of the surface air HCHO observations than either the GEIA or BEIS2 inventories; the simulation captures 71% of the observed spatial variance in the observations with a −10% bias. This result further demonstrates the consistency between the GOME and in situ observations.

[39] Our analysis focused on North America during summer but it can be readily extended to the globe. It could be used to map isoprene emissions from tropical ecosystems or to determine the seasonal pattern of isoprene emissions at northern midlatitudes. Following on the approach in section 2, care has to be taken to identify any additional VOCs besides isoprene that could make a significant contribution to the HCHO column. Outside of the growing season, longer-lived anthropogenic VOCs may become important and a more detailed inversion analysis would be required to relate the sources to the observed HCHO columns.

Appendix A: GEOS-CHEM Model Description

[40] The GEOS-CHEM global 3-D model of tropospheric chemistry is driven by assimilated meteorological data from

the GEOS of the NASA Data Assimilation Office (DAO) [*Schubert et al.*, 1993]. The 3-D meteorological data are updated every 6 hours; mixing depths and surface fields are updated every 3 hours. We use here GEOS fields for 1996 available with $2° \times 2.5°$ (latitude/longitude) resolution and 40 sigma levels in the vertical, extending up to 0.1 hPa. We retain the original horizontal resolution but keep only 26 vertical levels by merging levels in the stratosphere which provide negligible information relevant to HCHO. The lowest model layers are centered at approximately 50, 250, 600, and 1100 m for a box at sea level. A comprehensive description and evaluation of the GEOS-CHEM model for tropospheric O_3–NO_x–VOC chemistry is given by *Bey et al.* [2001], and improvements and application to regional air quality over North America during summer are given by *Fiore et al.* [2002]. We use here is version 4.4 of the GEOS-CHEM model. We initialize the GEOS-CHEM model in May 1996 with monthly mean values taken from another year [*Bey et al.*, 2001] and run the model forward in time through July 1996.

[41] The chemical mechanism is that of *Horowitz et al.* [1998] with minor updates [*Bey et al.*, 2001; *Fiore et al.*, 2002]. It includes detailed representation of oxidation pathways for five non-methane hydrocarbons (NMHCs) (ethane, propane, lumped $>C_3$ alkanes, lumped $>C_2$ alkenes, and isoprene). Numerical integration of the mechanism is done with a fast Gear solver [*Jacobson and Turco*, 1994]. In the present version we recycle by photolysis and reaction with OH the organic peroxides produced from isoprene oxidation, following the mechanism of *Lurmann et al.* [1986] and as discussed in section 2.1. Photolysis rates are computed using the Fast-J radiative transfer algorithm [*Wild et al.*, 2000] which includes Rayleigh scattering as well as Mie scattering by clouds. We use monthly averaged UV albedo fields from the study of *Herman and Celarier* [1997]. Aerosol scattering is included in the model by specifying AODs from a correlation with surface O_3, as described by *Fiore et al.* [2002].

[42] Gridded emission fields for anthropogenic NO_x and NMHCs over North America in 1985 are taken from the study of *Wang et al.* [1998] and are scaled to 1996 using national emission data. Biogenic hydrocarbon emissions include isoprene as discussed in the text plus small contributions from acetone and propene. Emissions of terpenes and methanol are not included; as discussed in the text, they are unlikely to make significant contributions to the HCHO column signal from GOME.

[43] **Acknowledgments.** For useful discussions of the ideas presented, we thank Alex Guenther (National Center for Atmospheric Research), Bryan Duncan (Harvard University, now at Ecole Polytechnique Federale de Lausanne, Switzerland), Yin-Nan Lee (Brookhaven National Laboratory), Tom Pierce and Robin Dennis (Environmental Protection Agency), and Robert Chatfield (NASA Ames). This work was supported by the NASA Atmospheric Chemistry Modeling and Analysis Program (ACMAP) and by the Atmospheric Chemistry Program of the U.S. National Science Foundation.

References

Altshuller, A. P., The production of carbon monoxide by the homogeneous NO_x-induced photooxidation of volatile organic compounds in the troposphere, *J. Atmos. Chem.*, *13*, 155–182, 1991.

Alvarado, A., E. C. Tuazon, S. M. Aschmann, J. Arey, and R. Atkinson, Products and mechanisms of the gas-phase reactions of OH radical and O_3 with 2-methyl-3-buten-2-ol, *Atmos. Environ.*, *33*, 2893–2905, 1999.

Atkinson, R., Gas-phase tropospheric chemistry of organic compounds, *J. Phys. Chem. Ref. Data Monogr.*, *2*, 13–46, 1994.

Atkinson, R., and J. Arey, Atmospheric chemistry of biogenic organic compounds, *Acc. Chem. Res.*, *31*, 574–583, 1998.

Balkanski, Y. J., D. J. Jacob, G. M. Gardiner, W. C. Graustein, and K. K. Turekian, Transport and residence times of tropospheric aerosol inferred from a global three-dimensional simulation of 210 Pb, *J. Geophys. Res.*, *98*, 20,573–20,586, 1993.

Betterton, E. A., Henry's law constants of soluble and moderately soluble organic gases: Effects of aqueous-phase chemistry, *Adv. Environ. Sci. Technol.*, *24*, 1–50, 1992.

Bey, I., et al., Global modeling of tropospheric chemistry with assimilated meteorology: Model description and evaluation, *J. Geophys. Res.*, *106*, 23,073–23,096, 2001.

Burrows, J. P., et al., The Global Ozone Monitoring Experiment (GOME): Mission concept and first scientific results, *J. Atmos. Sci.*, *56*, 151–175, 1999.

Chance, K., P. I. Palmer, R. J. D. Spurr, R. V. Martin, T. P. Kurosu, and D. J. Jacob, Satellite observations of formaldehyde over North America from GOME, *Geophys. Res. Lett.*, *27*, 3461–3464, 2000.

Dickerson, R. R., S. Kondragunta, G. Stenchikov, K. L. Civerolo, B. G. Doddridge, and B. N. Holben, The impact of aerosols on solar ultraviolet radiation and photochemical smog, *Science*, *278*, 827–830, 1997.

DOE, Emissions of greenhouse gases in the United States 1996, doe/eia-0573(96), Tech. Rep., Energy Inf. Admin., Off. of Integrated Anal. and Forecasting, U.S. Dept. of Energy, Washington, D. C. 20585, 1997.

Fiore, A. M., D. J. Jacob, I. Bey, R. M. Yantosca, B. D. Field, and J. Wilkinson, Background ozone over the United States in summer: Origin and contribution to pollution episodes, *J. Geophys. Res.*, *107*, 4279, doi:10.1029/2001JD000982, 2002.

Fried, A., et al., Photochemistry of formaldehyde during the 1993 Tropospheric OH Photochemistry Experiment, *J. Geophys. Res.*, *102*, 6283–6296, 1997.

Frost, G. J., et al., Comparison of box model calculations and measurements of formaldehyde from the 1997 North Atlantic Regional Experiment, *J. Geophys. Res.*, *107*(D12), 4060, doi:10.1029/2001JD000896, 2002.

Griffin, R. J., D. R. Cocker III, R. C. Flagan, and J. H. Seinfeld, Organic aerosol formation from the oxidation of biogenic hydrocarbons, *J. Geophys. Res.*, *104*, 3555–3567, 1999.

Guenther, A., et al., A global model of natural volatile organic compound emissions, *J. Geophys. Res.*, *100*, 8873–8892, 1995.

Guenther, A. C., T. Pierce, B. Lamb, P. Harley, and R. Fall, Natural emissions of non-methane volatile organic compounds, carbon monoxide, and oxides of nitrogen from North America, *Atmos. Environ.*, *34*, 2205–2230, 2000.

Harris, G. W., G. I. Mackay, T. Iguchi, L. K. Mayne, and H. I. Schiff, Measurements of formaldehyde in the troposphere by tunable diode laser absorption spectroscopy, *J. Atmos. Chem.*, *8*, 119–137, 1989.

Hatakeyama, S., K. Izumi, T. Fukuyama, H. Akimoto, and N. Washida, Reactions of OH with α-pinene and β-pinene in air: Estimate of global CO production and atmospheric oxidation of terpenes, *J. Geophys. Res.*, *96*, 947–958, 1991.

Herman, J. R., and E. A. Celarier, Earth surface reflectivity climatology at 340–380 nm from TOMS data, *J. Geophys. Res.*, *102*, 28,003–28,011, 1997.

Hirsch, R. M., and E. J. Gilroy, Methods of fitting a straight line to data: Examples in water resources, *Water Res. Bull.*, *20*, 705–711, 1984.

Horowitz, L. W., J. Liang, G. M. Gardner, and D. J. Jacob, Export of reactive nitrogen from North America during summertime: Sensitivity to hydrocarbon chemistry, *J. Geophys. Res.*, *103*, 13,451–13,476, 1998.

Jacobson, M. Z., and R. P. Turco, SMVGEAR: A sparse-matrix, vectorized Gear code for atmospheric models, *Atmos. Environ.*, *28*, 273–284, 1994.

Kamens, R. M., M. W. Gery, H. E. Jeffries, M. Jackson, and E. I. Cole, Ozone–isoprene reactions: Product formation and aerosol potential, *Int. J. Chem. Kinet.*, *14*, 955–975, 1982.

Kleindienst, T. E., et al., An intercomparison of formaldehyde techniques at ambient concentration, *Atmos. Environ.*, *22*, 1931–1939, 1988.

Kurosu, T. P., K. Chance, and R. J. D. Spurr, CRAG: Cloud Retrieval Algorithm for the European Space Agency's Global Ozone Monitoring Experiment, in Proceedings of the European Symposium of Atmospheric Measurements From Space, pp. 513–521, Eur. Space Agency, Paris, 1999.

Kuze, A., and K. V. Chance, Analysis of cloud top height and cloud coverage from satellites using the O_2A and B bands, *J. Geophys. Res.*, *99*, 14,481–14,491, 1994.

Lee, Y.-N., X. Zhou, and K. Hallock, Atmospheric carbonyl compounds at a rural southeastern United States site, *J. Geophys. Res.*, *100*, 25,933–25,944, 1995.

Lee, Y.-N., et al., Nashville/Middle Tennessee Ozone Study, *J. Geophys. Res.*, *103*, 22,449–22,462, 1998.

Li, Q., et al., Transatlantic transport of pollution and its effects on surface ozone in Europe and North America, *J. Geophys. Res.*, *107*(D13), 4166, doi:10.1029/2001JD001422, 2002.

Lurmann, F. W., A. C. Lloyd, and R. Atkinson, A chemical mechanism for use long-range transport acid deposition computer modeling, *J. Geophys. Res.*, *91*, 905–936, 1986.

Martin, R. S., H. Westberg, E. Allwine, L. Ashman, and B. Lamb, Measurement of isoprene and its atmospheric oxidation products in a central Pennsylvania deciduous forest, *J. Atmos. Chem.*, *13*, 1–32, 1991.

Martin, R. V., et al., An improved retrieval of tropospheric nitrogen dioxide from GOME, *J. Geophys. Res.*, *107*(D20), 4437, doi:10.1029/2001JD001027, 2002.

Orlando, J. J., B. Nozière, G. S. Tyndall, G. E. Orzechowska, S. E. Paulson, and Y. Rudich, Product studies of the OH- and ozone initiated oxidation of some monoterpenes, *J. Geophys. Res.*, *105*, 11,561–11,572, 2000.

Palmer, P. I., et al., Air mass factor formulation for spectroscopic measurements from satellites: Application to formaldehyde retrievals from the Global Ozone Monitoring Experiment, *J. Geophys. Res.*, *106*, 14,539–14,550, 2001.

Paulson, S. E., and J. H. Seinfeld, Development and evaluation of a photooxidation mechanism for isoprene, *J. Geophys. Res.*, *97*, 20,703–20,715, 1992.

Pierce, T., C. Geron, L. Bender, R. Dennis, G. Tonnesen, and A. Guenther, Influence of increased isoprene emissions on regional ozone modeling, *J. Geophys. Res.*, *103*, 25,611–25,629, 1998.

Richter, A., and T. Wagner, Diffuser plate spectral structures and their influence on GOME slant columns, Tech. Rep., Inst. Environ. Phys., Univ. Bremen and Inst. Environ. Phys., Univ. Heidelberg, 2001.

Richter, A., F. Wittrock, A. Ladsttter-Weibenmayaer, and J. P. Burrows, GOME measurements of stratospheric and tropospheric BrO, *Adv. Space. Res.*, *29*(11), 1667–1672, 2002.

Riemer, D., et al., Observations of nonmethane hydrocarbons and oxygenated volatile organic compounds at a rural site in the southeastern United States, *J. Geophys. Res.*, *103*, 28,111–28,128, 1998.

Rudich, Y., R. Talukdar, J. B. Burkholder, and A. R. Ravishankara, Reaction of methylbutenol with hydroxyl radical: Mechanism and atmospheric implications, *J. Phys. Chem.*, *99*, 12,188–12,194, 1995.

Schubert, S. D., R. B. Rood, and J. Pfaendtner, An assimilated data set for Earth Science applications, *Bull. Am. Meteorol. Soc.*, *74*, 2331–2342, 1993.

Shepson, P. B., D. R. Hastie, H. I. Schiff, M. Polizzi, J. W. Bottenheim, K. Anlauf, G. I. Mackay, and D. R. Karecki, Atmospheric concentrations and temporal variations of C_1–C_2 carbonyl compounds at two rural sites in central Ontario, *Atmos. Environ.*, *25*, 2001–2015, 1991.

Sprengnether, M., K. L. Demerjian, N. M. Donahue, and J. G. Anderson, Product analysis of the OH oxidation of isoprene and 1,3-butadiene in the presence of NO, *J. Geophys. Res.*, *107*(D15), 4268, doi:10.1029/2001JD000716, 2002.

Thornton, J. A., et al., Ozone production rates as a function of NO_x abundances and HO_x production rates in the Nashville urban plume, *J. Geophys. Res.*, *107*(D12), 4146, doi:10.1029/2001JD000932, 2002.

Wang, Y., D. J. Jacob, and J. A. Logan, Global simulation of tropospheric O_3-NO_x-hydrocarbon chemistry, 1, Model formulation, *J. Geophys. Res.*, *103*, 10,713–10,726, 1998.

Wild, O., X. Zhu, and M. J. Prather, Fast-J: Accurate simulations of in- and below-cloud photolysis in tropospheric chemistry models, *J. Atmos. Chem.*, *37*, 245–282, 2000.

Xu, M., J. Q. Chen, and B. L. Brookshire, Temperature and its variability in oak forests in the southeastern Missouri Ozarks, *Clim. Res.*, *8*, 209–223, 1997.

K. Chance and T. P. Kurosu, Harvard-Smithsonian Center for Astrophysics, Cambridge, MA, USA.

A. M. Fiore, D. J. Jacob, R. V. Martin, and P. I. Palmer, Division of Engineering and Applied Sciences, Harvard University, Cambridge, MA, USA. (pip@io.harvard.edu)

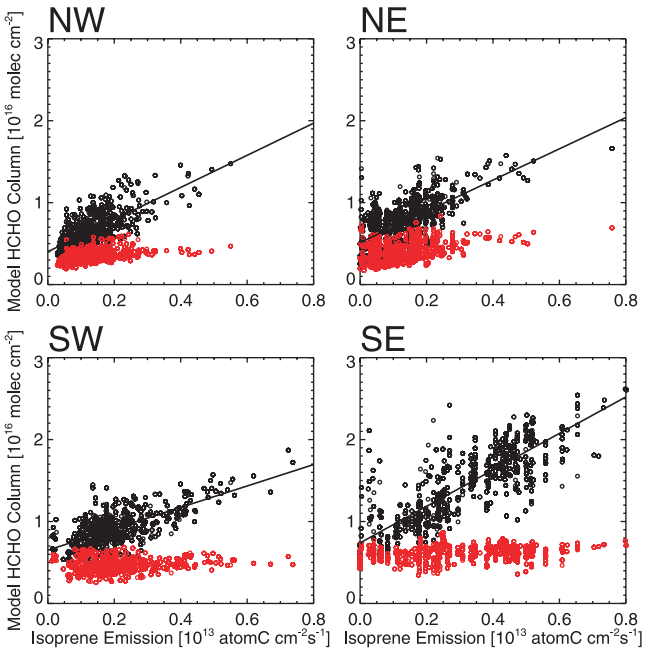

Figure 3. Relationship between isoprene emissions and HCHO columns in the GEOS-CHEM model for July 1996 over North America (25°–50°N, 65°–130°W) at 10–12 LT, partitioned by quadrants with longitudinal and latitudinal divides at 100°W and 40°N. Model values are sampled along the ensemble of GOME orbit tracks during July 1996. Cloud fraction data from GOME [*Kurosu et al.*, 1999] have been used to filter out scenes with >40% cloud cover. The linear-least squares fit lines are shown and the corresponding statistical data are given in Table 3. The red data points represent HCHO columns from sources other than isoprene, as determined from a sensitivity simulation without isoprene emissions.

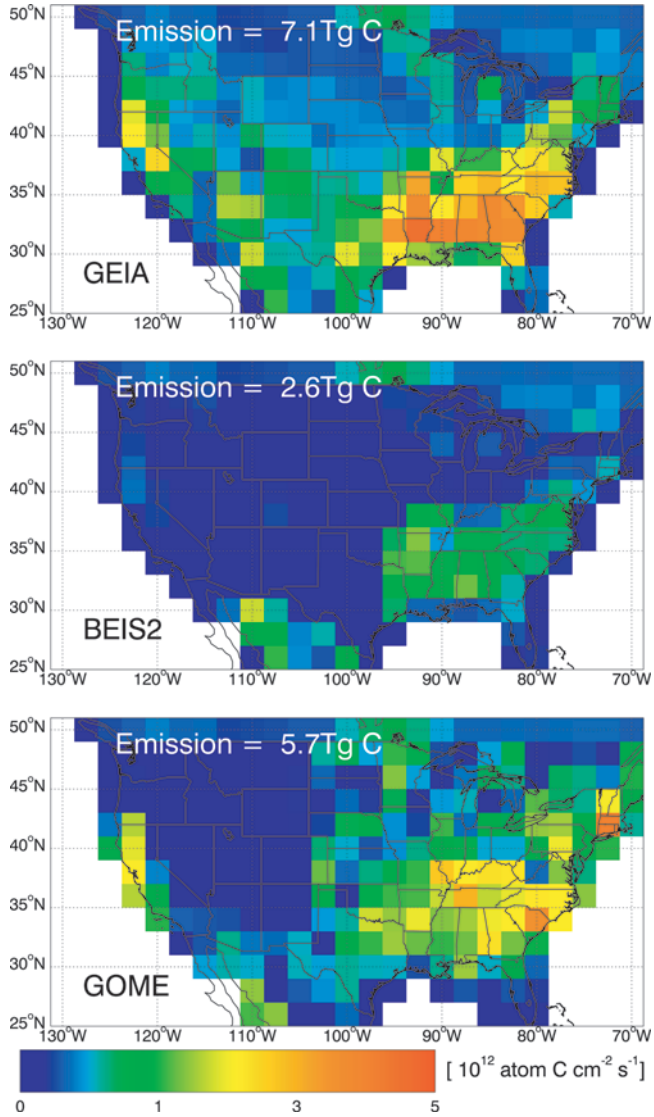

Figure 4. Monthly mean isoprene emission fluxes over North America for July 1996 from the GEIA and BEIS2 inventories and as retrieved from the GOME HCHO column observations. Total isoprene emissions during July over the domain is shown inset.

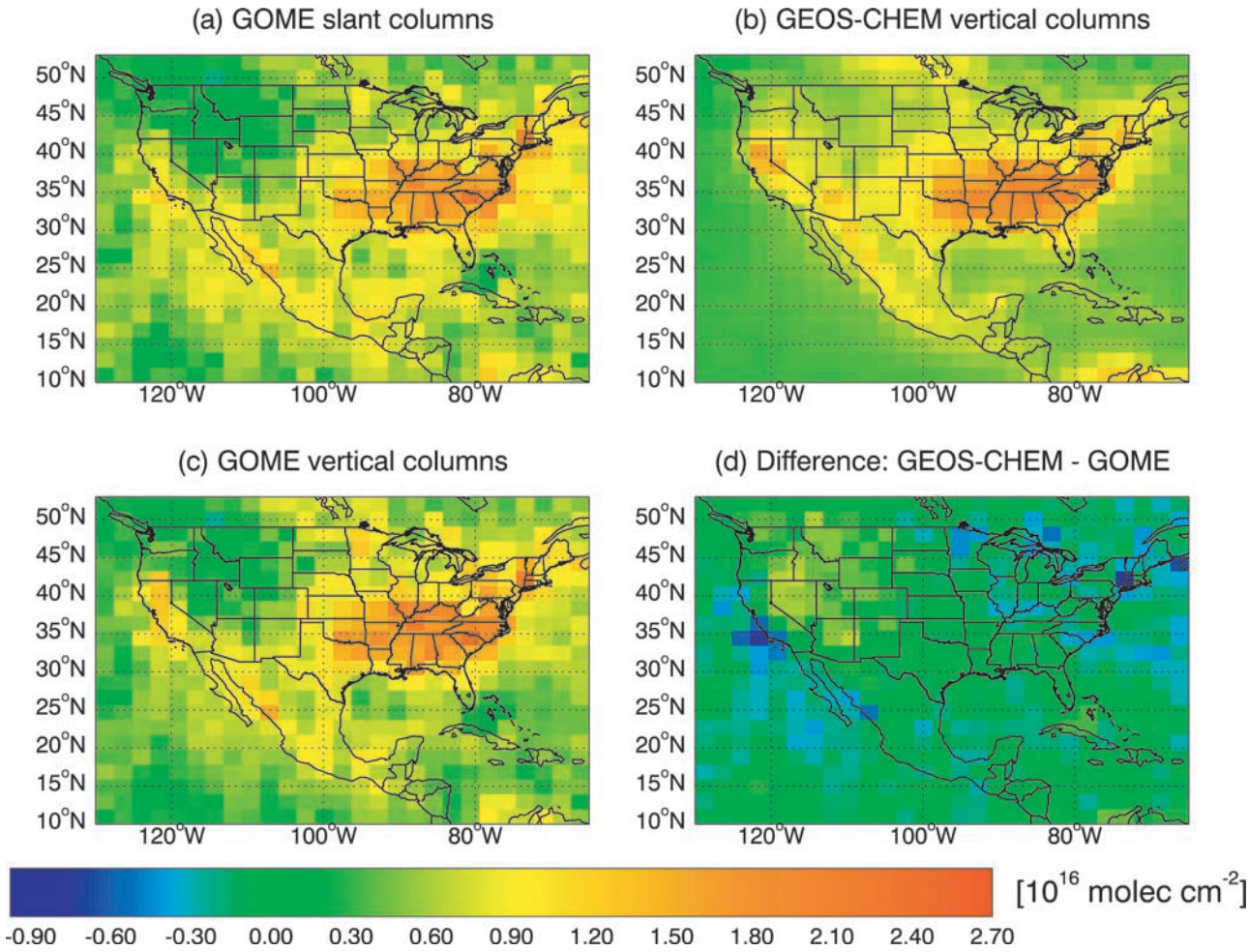

Figure 5. Mean HCHO columns over the United States for July 1996 on a 2° × 2.5° grid. (a) Observed slant columns from GOME [*Chance et al.*, 2000]. (b) Vertical columns from the GEOS-CHEM global 3-D model. (c) Observed vertical columns from GOME after application of the AMF. (d) Differences between modeled and observed vertical columns. Both model and observations are for 10ndash;12 LT and for cloud cover <40% [*Kurosu et al.*, 1999].

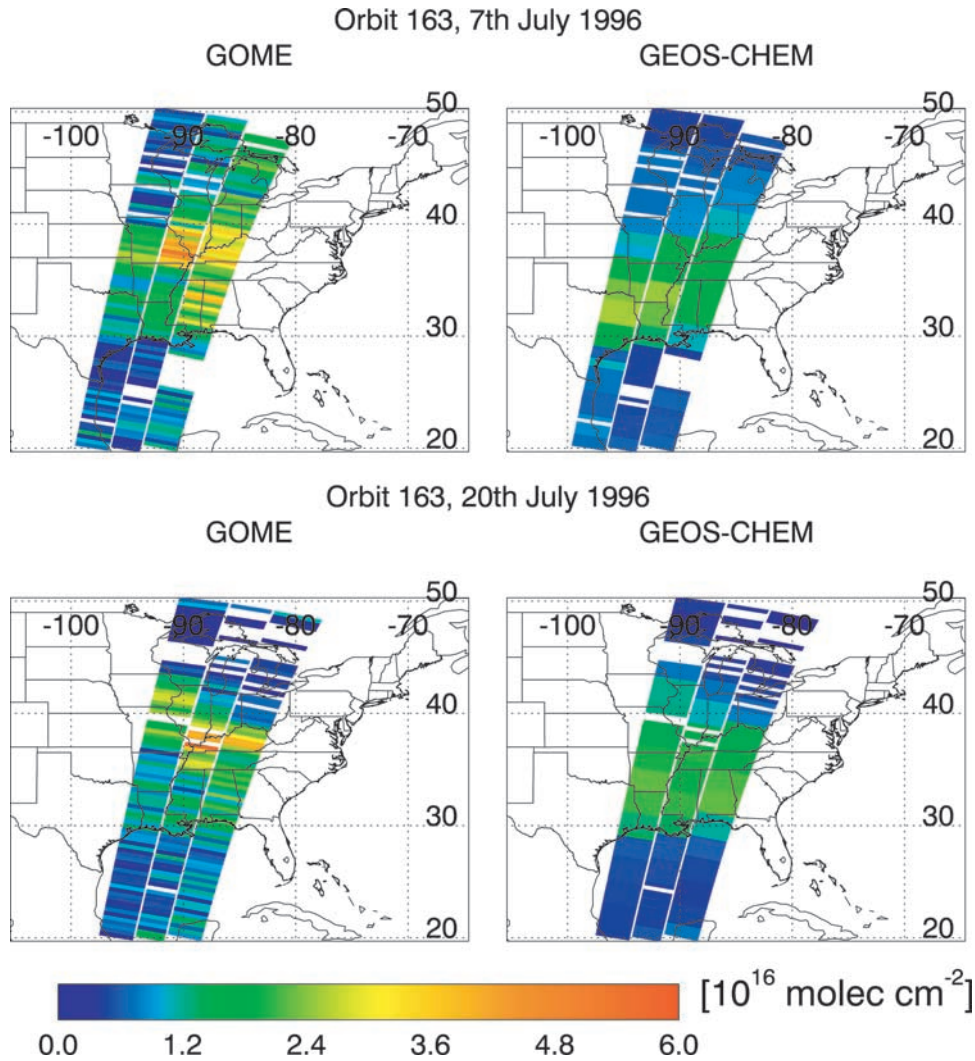

Figure 7. GOME HCHO vertical columns for two sample orbits over North America during July 1996. The left panels are the observed vertical columns and the right panels are the corresponding vertical columns from the GEOS-CHEM model at 10–12 LT. Data with GOMECAT [*Kurosu et al.*, 1999] cloud fraction values >0.4 have been omitted from both modeled and observed scenes.